Flow Field Influence Analysis of Combination Intake Port to Port and In-Cylinder for a Four-Valve Diesel Engine

D. W. Jia[1], X. W. Deng[1], Y. Wang[2] and J. L. Lei[1,†]

[1.]*Yunnan Key Laboratory of Internal Combustion Engine, Kunming University of Science and Technology, Kunming 650500, China*
[2.]*Yunnan Yuntong Judicial Expertise Center, Kunming 650224, China*

† *Corresponding Author Email: 22972489@qq.com*

ABSTRACT

Intake port structure directly affects the flow characteristics and combustion process of diesel engine, and then affects the comprehensive performance of diesel engine. To the intake ports of a four-valve direct injection diesel engine, the flow characteristics are analyzed on the four combined intake ports : (1) helical (left) and tangential (right), (2) tangential (left) and helical (right); (3) helical (left) and helical (right); and (4) tangential (left) and tangential (right).And the influence of air flow in four combined intake ports to in-cylinder gas flow is also analyzed. Results show that the helical and tangential combination intake ports flow velocity increases with the valve lift increases, and small turbulence arises at the valve guide lug, and the intake flow velocity of the minimum cross-section of the junction of the guiding section and the helical section is the maximum. The air flow in- cylinder moves from top cylinder head bottom to the cylinder bottom, the air flow is enlarged gradually by the small-scale irregular swirl, which eventually converges to a single swirl. The turbulence kinetic energy is very big when the air is just entering the cylinder, the flow space expands rapidly, and the dissipation of turbulent kinetic energy is very significant with the gas moves to the bottom of the cylinder.

Keywords: Four-valve diesel engine; Combined intake ports; Air flow in intake ports; Air flow in-cylinder.

1. INTRODUCTION

The combustion efficiency, fuel consumption and emissions of diesel engine are closely related to the formation and flow of the air and fuel mixture, flow characteristics are critical in determining the overall performance of diesel combustion systems. At the same time, when the diesel engine is operating at low speed, the atomization effect of the fuel is poor, and a strong intake vortex is required to increase the mixing effect of the fuel-air mixture. At high-speed operating conditions, it is necessary to reduce the intake resistance and increase the intake air amount. Therefore, it is necessary to adopt a suitable intake system structure to improve the intake flow of diesel engine, and the four-valve is the main structure of the high-speed direct injection diesel engine intake system. Therefore, the study of the two intake ports in the four-valve intake system structure and its combination method have become the core and key for fuel combustion system matching (Yufeng, *et al.*,2001).

The intake port shape of the diesel engine mainly includes helical and tangential port. In the four-valve diesel engine, the four combined intake ports are widely used: spiral and tangential, tangential and spiral, spiral and spiral, and tangential and tangential. So it is great significance for systematic analysis the air flow field and its laws of the combined intake port and in the cylinder, which is the development of high-performance diesel engines, matching combustion chambers and combustion systems (Kawaguchi, A.,*et al.*,2009, Andreatta, É. C.,*et al.*,2008).

Tests and simulation methods were often used to study the flow field in the intake port and in-cylinder of diesel engines (Deqing *et al*., 2002,Cui,L.,2015, Micklow G J,*et al.*,2007, Ma Hongwei,*et al.*,2013, Wang Tianyou,*et al.*,2008, Stiehl, R.,*et al.*,2016).At the same time, the intake port design method of some non diesel engine was also studied (Yuguo, *et al.*,2014, Thangavel *et al.*, 2016) ,at last , the ports were optimized(Sun, Y. *et al.*,2015, Son, J. W.,*et al.*,2004). Because the air flow in-cylinder was difficult to experiment research at the same time, the three-dimensional models of four different combined intake ports with spiral and tangential port were established. The

FIRE module of AVL software was used to simulate the flow field in the intake port and in-cylinder, which provided ideas for intake port design.

2. SIMULATION MODEL AND VERIFICATION

2.1 Basic Parameters of Research Object

The intake ports for research are a four-valve two-cylinder high-pressure common-rail diesel engine of passenger car. The basic parameters of diesel engine are shown in Table 1.

**Table 1 Basic parameters of the diesel engine**

Name	Parameters
bore×stroke/mm×mm	80×92
maximum valve lift/mm	8
compression ratio	16.5
combustion chamber type	ω type
maximum torque/N·m	125
maximum torque speed/r/min	2200
rated power/kW	41

2.2 Establishment of Simulation Model

（1）3D solid model

The 3D intake port model is designed by and the location in the cylinder head, the solid model of intake port was established by using the Unigraphics (UG) software 8.0, and the specifications of the intake port listed in Table 2.

According the Table 2, the four schemes of the combination intake ports are built, and the 3D model are shown in Fig. 1. To analyze the flow field accurately, the same volume of the air in single tangential or helical port is necessary.
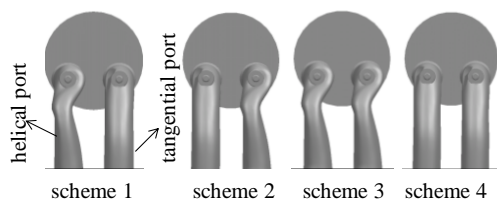

Fig. 1. Combined intake ports.

（2）Flow simulation model

To simulate the steady-state flow of the intake port, the simulation model is built in Fig. 2. And all pars are meshed by FAME Hybrid of the AVL FIRE pre-treatment meshed function module, and the meshes of the key pars were refining, such as the valve and valve seat. The total number of meshes is about 570,000, and the hexahedral grid accounts for about 90%.

（3）Control equation

The intake process of the diesel engine follows the continuity equation of the fluid motion, the law of conservation of momentum and conservation of energy. At the same time, the turbulent motion of the intake air is used by k-ε double function mode.
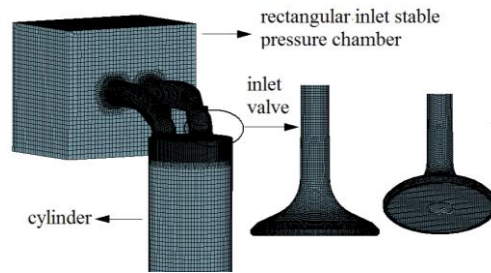
Fig. 2. Intake port analysis model.

（4）Boundary condition

Inlet boundary conditions: the constant-pressure-differentia of the inlet and outlet intake port is used. The total pressure is 100 kPa, the intake port temperature is 293.15 K, and the turbulent kinetic energy is 1 m^2/s^2.

Outlet boundary conditions: the cylinder outlet pressure differential is set to static pressure, which was 6.5 kPa at small valve lifts, and 2.5 kPa at high valve lifts.

Cylinder wall boundary conditions: the standard wall function is used on the wall surface with no-slip, adiabatic, and fixed temperature values.

2.3 Simulation Model Validation
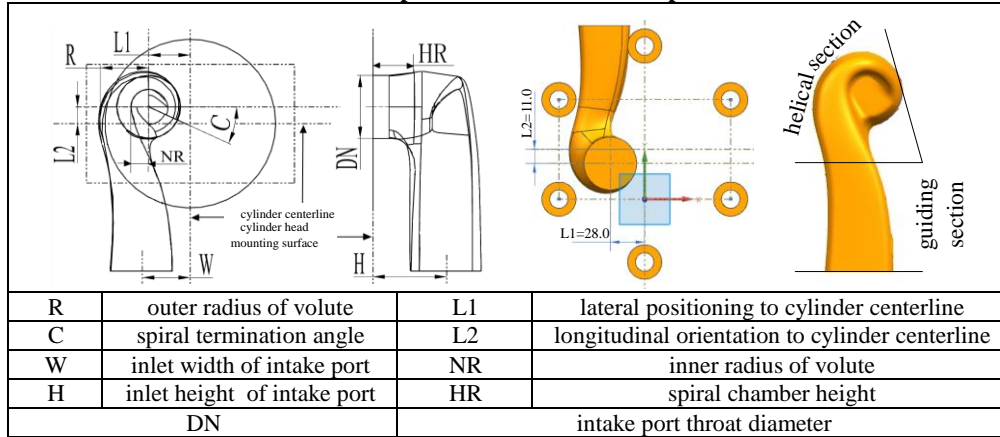
（1）Steady-state flow bench

The port steady flow simulation experiment is used to simulate the actual intake conditions of the diesel engine, which is used to evaluate flow characteristics and vortex formation capabilities of the intake port. It provides important test date for the development of the diesel engine air intake system and the formation of combustible air-fuel mixture in the cylinder. It is also the main method to validate different intake port simulation models. The actual air mass and vane anemometer speed are obtained by the experiment, and then the flow coefficient (μ) (the ration of actual air mass to theoretical air mass) and swirl ratio (SR) (the ration of vane anemometer speed to diesel engine simulation speed) are calculated [5].

The steady-state flow test bench is shown in Fig. 3, it is composed of a tachometer, an orifice flowmeter, and a vane anemometer, and other components. The experiment method is the same as the simulation method (constant pressure differentia). The simulation cylinder is 2.5 D, and the blade distant to cylinder head top is 1.75 D (D-cylinder diameter).

（2）Model validation

The flow coefficient and swirl ratio of the simulation and experiment results are compared, which is used to validate the rationality simulation of model construction with an example of scheme2 .The results are shown in Fig. 4 and Fig. 5.

Table 2 Specifications of the intake port

R	outer radius of volute	L1	lateral positioning to cylinder centerline
C	spiral termination angle	L2	longitudinal orientation to cylinder centerline
W	inlet width of intake port	NR	inner radius of volute
H	inlet height of intake port	HR	spiral chamber height
DN			intake port throat diameter
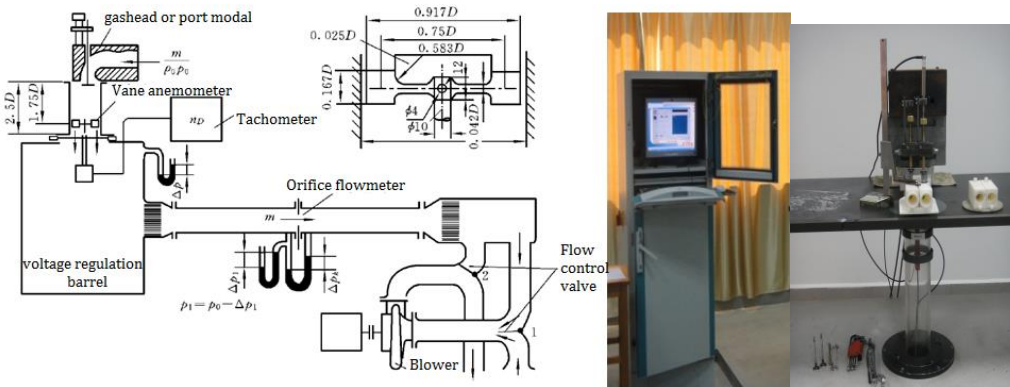
Fig. 3. Steady-state flow bench of intake port.
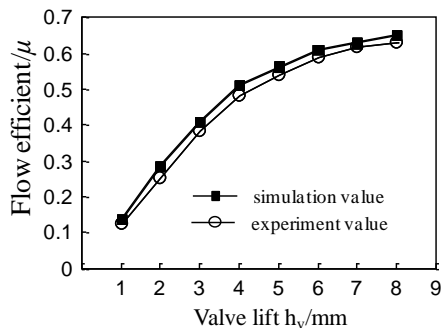
Fig. 4. Change of flow coefficient with valve lift in scheme 2.
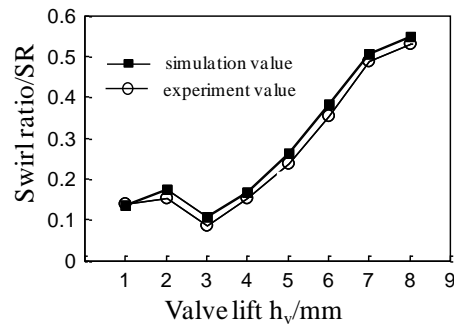
Fig. 5. Change of swirl ratio with valve lift in scheme 2.

As shown in Fig. 4, the flow coefficient increases with valve lift increases. The maximum deviation between experiment and simulation values is 8.5% when the valve lift is 2 mm.

As shown in Fig. 5, it can be seen that the swirl ratio fluctuates slightly when the valve lift is 3 mm. The main reason is that the cross-section area of intake flow is small when the valve lift is small, the throttling effect is obvious and the turbulent intensity near the throat of the port increases. Then, the swirl ratio is on the rise with the valve lift increases, and the maximum error between the simulate and the experiment value is less than 5%, which indicates that the simulation model is basically reasonable and can be used to analyze

different schemes.

3. FLOW FIELD ANALYSIS OF INTAKE PORT

According to the simulation parameters above, all the boundary conditions are set up in the FIRE software, the flow field of the intake port is obtained after simulation. And the flow field of different schemes is analyzed when the valve lift is 2, 4, 6 and 8 mm.

3.1 The Flow Field Analysis of Scheme1 and Scheme2
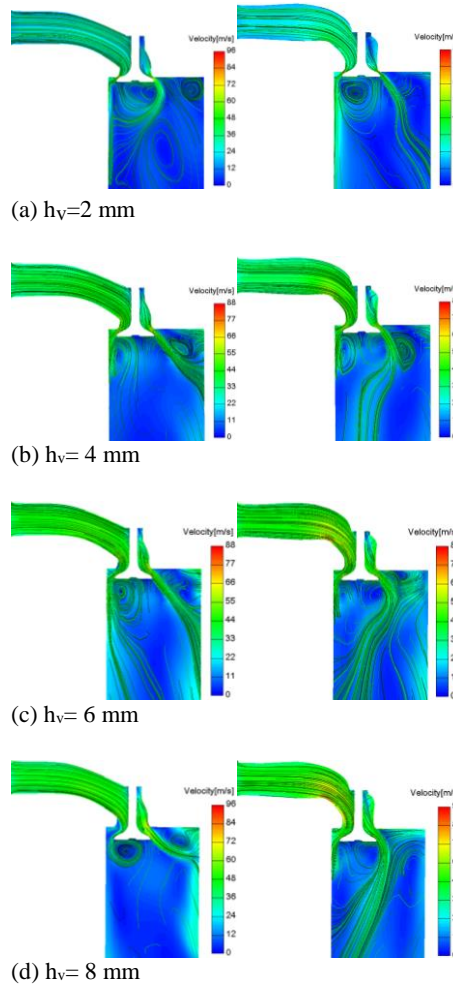
The contours of the flow velocity of scheme1 and

scheme2 are shown in Fig. 6 and Fig. 7.

(a) h_v=2 mm

(b) h_v= 4 mm

(c) h_v= 6 mm

(d) h_v= 8 mm
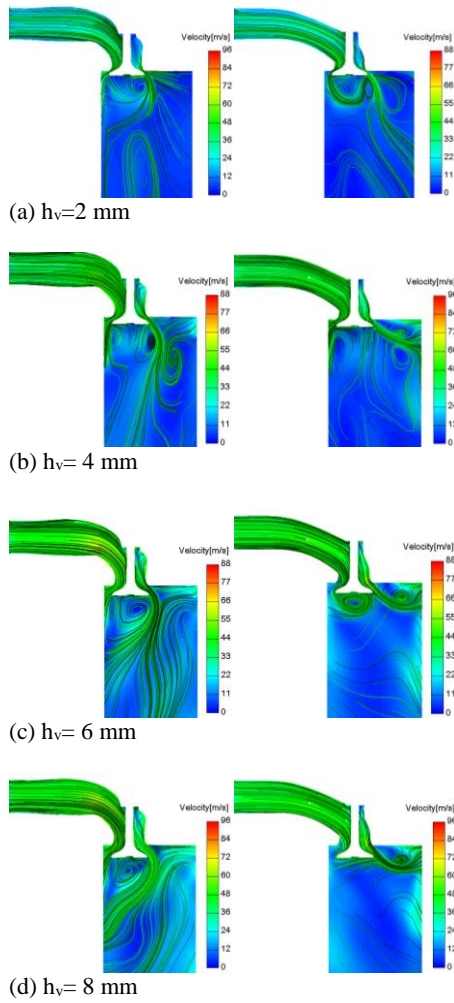
Fig. 6. Air flow velocity contour of scheme1.

As shown in Fig. 6, when the valve opening increases from small to large, the cross-sectional area between the valve and the valve seat increases, and the air flow resistance decreases. The air flows into the in-cylinder quickly because of pressure difference between intake port and in-cylinder. The small turbulence is caused by low flow velocity at the boss of the valve guide; there is even a phenomenon of detention caused by a small change in speed. The maximum air velocity of the helical port occurs at the bevel edge of the valve when the valve lift is small. When the valve lift h_v=8 mm, the maximum air flow velocity occurs at the minimum cross-section of the guiding section and the helical section of the helical intake port. When the valve lift of the tangential port is small, the air flow velocity near the valve is more uniform; when the valve lift is large, the air flow velocity near the exhaust side is faster, and the maximum velocity of the air flow occurs between the valve and the valve seat ring. At the same valve lift, the air in the spiral port flows into cylinder along the cylinder wall and the area near the centerline of the cylinder. At the same time, the air in the tangential port flows

tangentially into cylinder, most of the air flow to the bottom of the cylinder and a small part of the air forms a small vortex with the cylinder head after hitting the cylinder wall.

(a) h_V=2 mm

(b) h_v= 4 mm

(c) h_v= 6 mm

(d) h_v= 8 mm

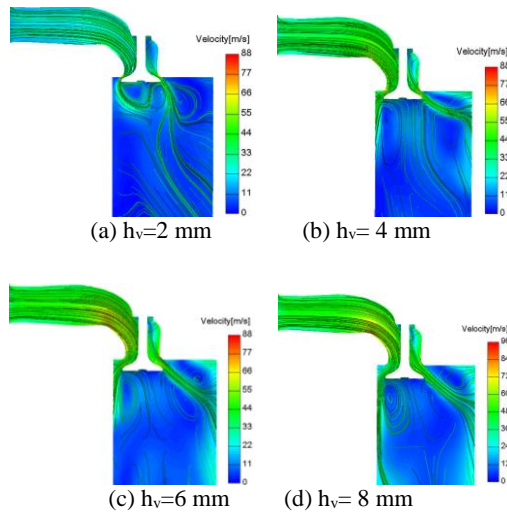**Fig. 7. Air flow velocity contour of scheme2.**

As shown in the Fig. 7, the maximum flow velocity and position of in the intake port are similar to those of shceme1, and the values of the flow velocity are also very small difference.

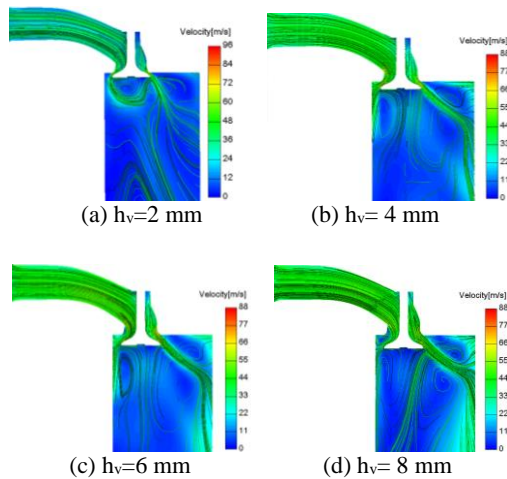### 3.2 Flow Field Analysis of Scheme3 and Scheme4

Because of the combined intake port of the scheme3 and scheme4 are composed of the helical and helical ports, tangential and tangential ports, respectively. The flow field analysis of the single helical port or tangential port is selected to represent to scheme3 or scheme4.

As shown in Fig. 8, when the air in the spiral intake port passes through the valve, some of the air flows rapidly along the inclined surface of valve and collides with the wall surface and then flows into the bottom of the cylinder. The other air below the valve forms a certain regular vortex near the centerline area after some air collides with cylinder wall.

(a) h_v=2 mm   (b) h_v= 4 mm

(c) h_v=6 mm   (d) h_v= 8 mm

Fig. 8. Air flow velocity contour of scheme3.

(a) h_v=2 mm   (b) h_v= 4 mm

(c) h_v=6 mm   (d) h_v= 8 mm

Fig. 9. Air flow velocity contour of scheme4.

As shown in Fig. 9, , most of the air in the tangential port flows tangentially into the side wall away from the cylinder inner wall along the port inner wall and the valve inclined surface, and a small part air flows into near the cylinder wall side. The air velocity changes little with the valve opening.

4. FLOW FIELD ANALYSIS IN-CYLINDER

To analyze the flow filed in-cylinder, the cylinder center line of the cylinder is defined as Z direction, and the top surface of cylinder is positive, and the following is negative. The flow field of different cross-section is analyzed with different valve lift, such as Z=-5, -35 and -65 mm. The turbulent kinetic energy is also analyzed at different cross-section, such as Z=- 5, -45 and -85 mm.

4.1 Flow Field Analysis In-Cylinder Corresponding to Scheme1

The air flow velocity of different cross-section in-cylinder with different valve lift is shown in Fig. 10

When h_v=2 mm and 4 mm, one or two small-scale vortex near the cylinder wall are formed between the spiral and tangential intake port at the section Z=-5 mm. And the anti-clockwise vortex from the spiral port to the tangential port near the cylinder wall is formed because of the collision and interference of the intake air flow to cylinder. And a clockwise vortex is formed at the edge of the spiral port when the intake air flow hits the cylinder wall and returns, which encounters the tangential inlet air flow. The intake air flow of the spiral and tangential port collides at the valve outlet, and two vortexes near the cylinder centerline are formed, resulting in the loss of intake air flow. When h_v=6 and 8 mm, the intake air flow velocity in the tangential port increases, and the new vortex is formed under the combined action of the cylinder wall and spiral air intake flow.

Comparing the (a), (b), (c) and (d), when the valve lift h_v= 2 and 4 mm, the numbers of chaotic vortexes decrease with the increase of cross-section distance. When h_v=6 mm, the small vortexes in the cylinder gradually form larger vortexes. When h_v=8 mm, a vortex about the same size as the diameter of the cylinder is formed near the cylinder centerline with the increase of the cross-section distance, which shows that the air is more evenly distributed in the cylinder.

When h_v = 2, 4, 6, and 8 mm, the distribution of turbulent kinetic energy in the cylinder is shown in Fig. 11. It can be seen that the maximum turbulent energy of the air flow appears at the slope edge area of the valve when the section Z=-5 mm, but the distribution position of turbulent energy is unstable. With the increase of the cross-section distance, the air quickly flows into the cylinder rapidly and diffuses rapidly, and irregular small-scale vortex diffuses and merges, eventually forming a swirl around the center line of the cylinder. At the same time, the turbulent kinetic energy dissipation is very significant with the air moving towards to the cylinder bottom. The irregular vortexes expand obvious and converge gradually into a single vortex in the process of moving from 1/2 stroke cross-section to cylinder bottom.

4.2 Flow Field Analysis In-Cylinder Corresponding to Scheme2

The air flow velocity of different cross-section in-cylinder with different valve lift is shown in Fig. 12 When the cross-section Z=-5 mm, several vortexes are formed near the outlet of the port. With the increase of the cross-section distance, the numbers of vortex gradually decrease and vortex gradually increases. Due to the flow interference between the tangential and helical intake ports, there are two or three small-scale vortexes with different swirling directions. At last, two large-scale vortexes are formed on the side of the exhaust valve, which are parallel to the cylinder centerline.

Comparing the (a), (b), (c) and (d), it can be seen that with the increase of valve lift and cross-section distance, the small vortex flows clockwise in
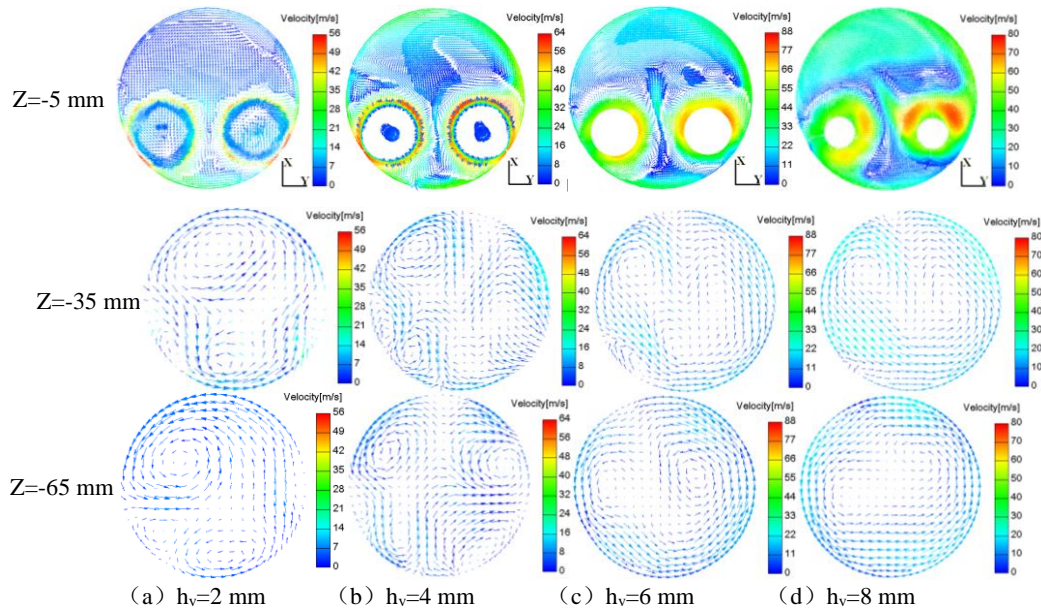
（a）h_v=2 mm　　（b）h_v=4 mm　　（c）h_v=6 mm　　（d）h_v=8 mm

Fig. 10. Air velocity vectors at different cylinder section with different valve lifts of shemen1.

（a）h_v=2 mm　　（b）h_v=4 mm　　（c）h_v=6 mm　　（d）h_v=8 mm
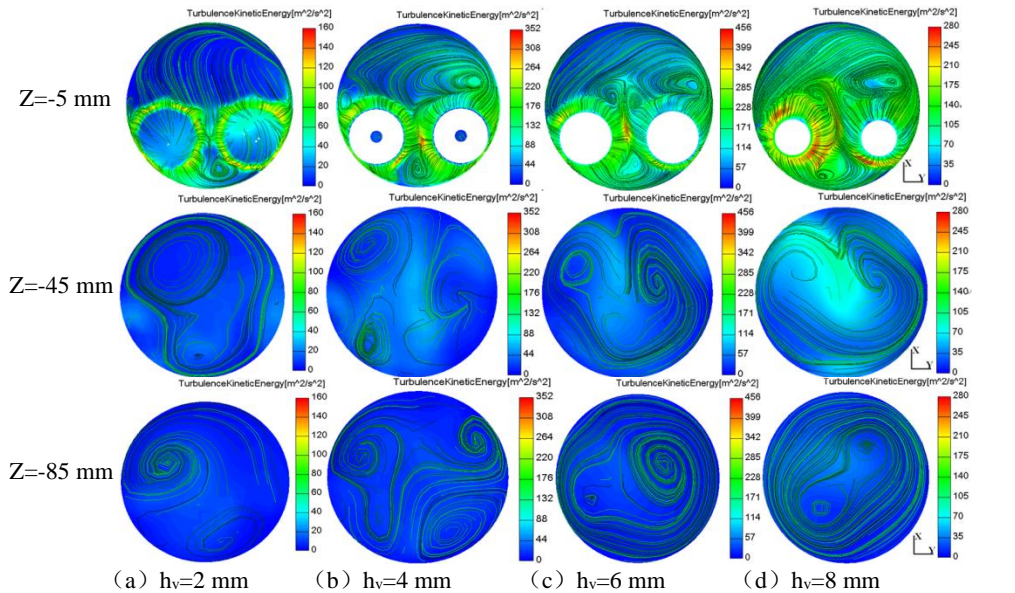
Fig. 11. Turbulent kinetic energy at different cylinder section with different valve lifts of shemen1.

cylinder, and the vortex near the exhaust valve side is almost the same size as the cylinder diameter.

When h_v = 2, 4, 6, and 8 mm, the distribution of turbulent kinetic energy in the cylinder is shown in Fig. 13. The distribution of turbulent kinetic energy in the cylinder is relatively uniform, and the turbulent energy near the cylinder wall is large because of the airflow collides severely with the cylinder wall. As the valve lift increases, several vortexes in the cylinder are gradually merge into a vortex and its rotation center is close to the exhaust valve side. The irregular vortexes expand obvious, disappears, and converge gradually into a single vortex in the process of moving from 1/2 stroke cross-section to cylinder bottom.

4.3 Flow Field Analysis In-Cylinder Corresponding to Scheme3

The air flow velocity of different cross-sections in-cylinder with different valve lift is shown in Fig. 14.

When cross-section Z=-5 mm, many small-scale vortexes are generated in the opposite direction, and two different sizes of vortexes are formed near the cylinder wall of the two valve edges, one of which is about half the cylinder diameter, and the other is very small.

Comparing the (a), (b), (c) and (d), when the cross-section Z = -35, -65 mm, the air flow in the cylinder is relatively regular. When the valve lift $_v$
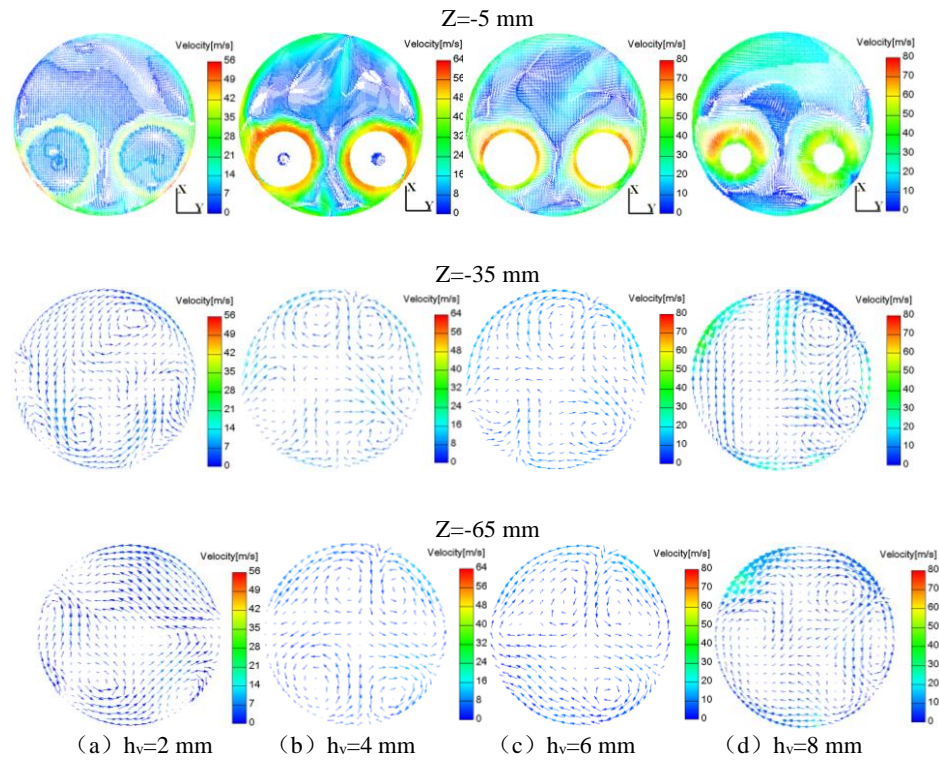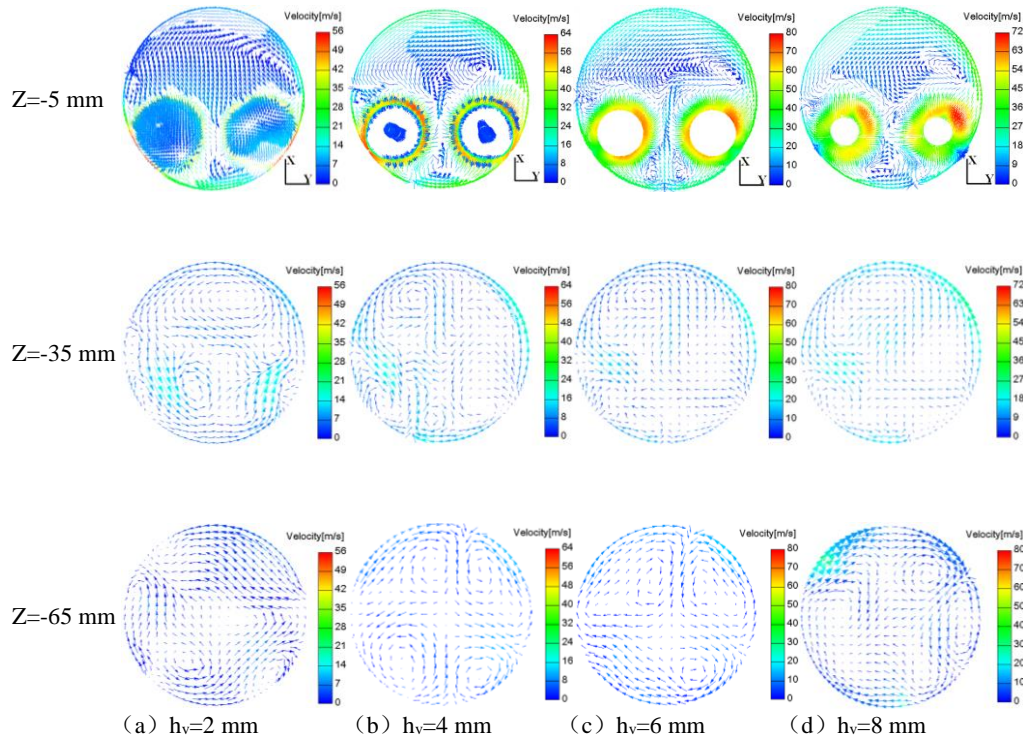
Z=-5 mm

Z=-35 mm

Z=-65 mm

（a）h_v=2 mm   （b）h_v=4 mm   （c）h_v=6 mm   （d）h_v=8 mm

Fig. 12. Air velocity vectors at different cylinder section with different valve lifts of shemen2.

Z=-5 mm

Z=-45 mm

Z=-85 mm

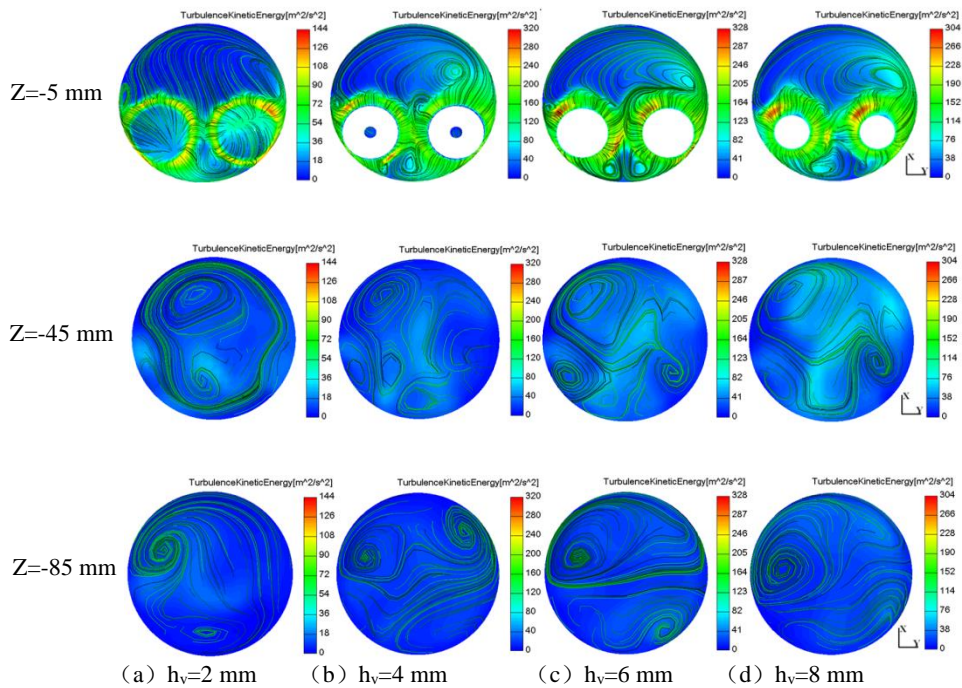（a）h_v=2 mm   （b）h_v=4 mm   （c）h_v=6 mm   （d）h_v=8 mm
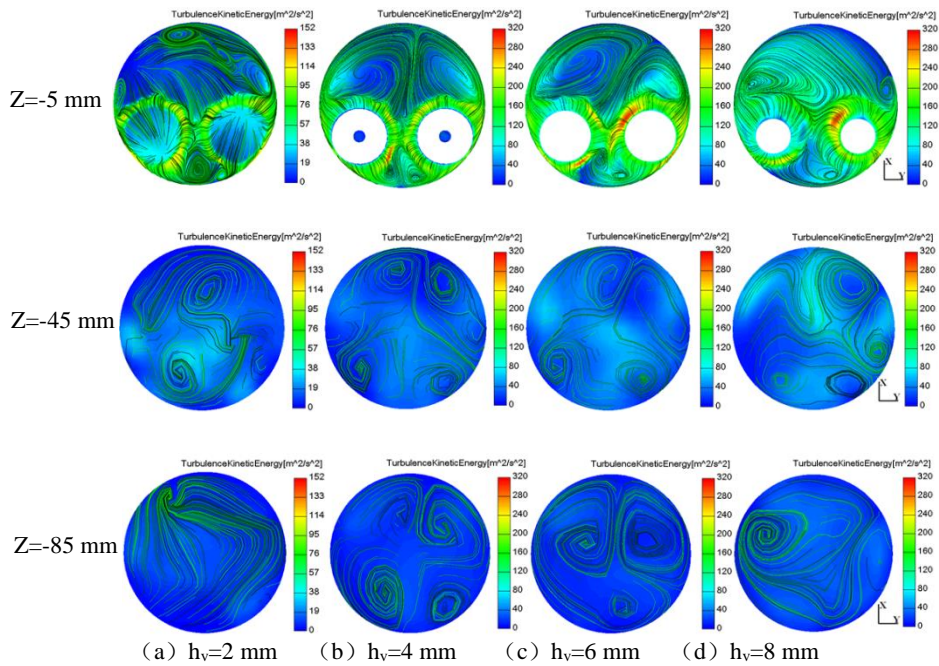
Fig. 13. Turbulent kinetic energy at different cylinder section with different valve lifts of shemen2.

h= 2 and 6 mm, two or three similar size vortexes are formed, and when the valve lift h_v=8 mm, the air in the cylinder is gradually merged under the left side of the spiral port, and the large vortex center is parallel to the cylinder centerline.

When h_v = 2, 4, 6, and 8 mm, the distribution of turbulent kinetic energy in the cylinder is shown in Fig. 15. It can be seen from the figure that the air turbulent kinetic energy of different cross-section in the cylinder is unevenly distributed, and the

Fig. 14. Air velocity vectors at different cylinder section with different valve lifts of shemen3.

Fig. 15. Turbulent kinetic energy at different cylinder section with different valve lifts of shemen3.

turbulent kinetic energy of the intake port is larger and the side of the exhaust side is smaller. The vortex near the cylinder top is no rule, a single vortex near the center of the intake valve is formed when the vortex is close to cylinder bottom and the valve lift $h_v=8$ mm. The irregular small vortexes gradually expand, disappear and converge into a single vortex from the 1/2 stroke cross-section to the cylinder bottom.

4.4 Flow Field Analysis In-Cylinder Corresponding to Scheme4

The air flow velocity of different cross-sections in-cylinder with different valve lift is shown in Fig. 16. When the cross-section Z = -5 mm, many vortexes
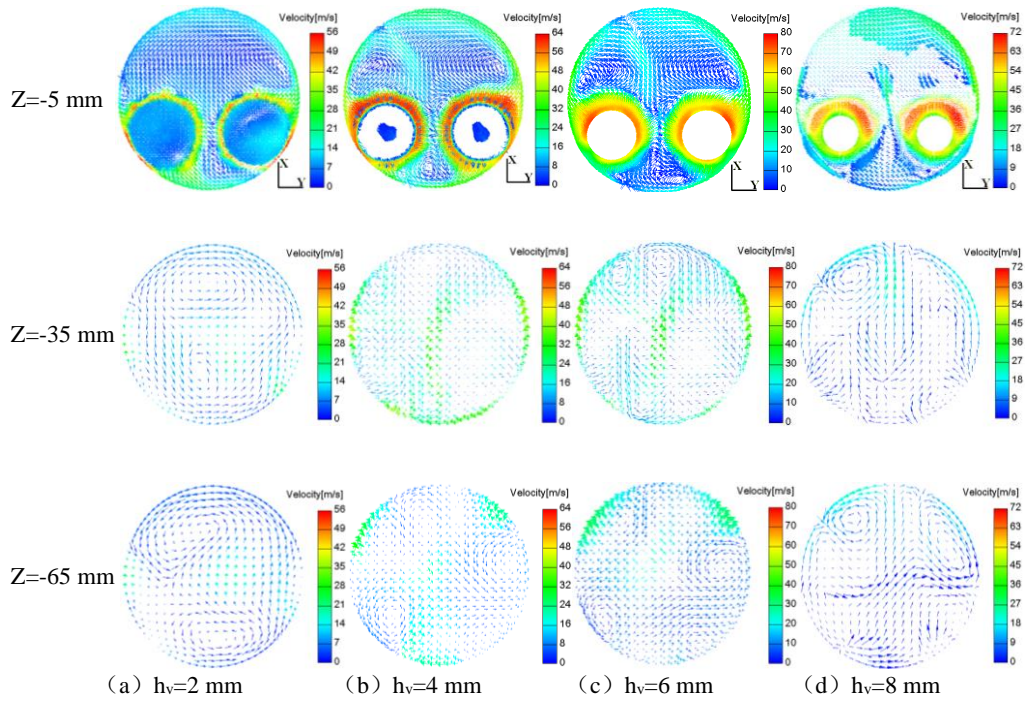
（a）h_v=2 mm   （b）h_v=4 mm   （c）h_v=6 mm   （d）h_v=8 mm

Fig. 16. Air velocity vectors at different cylinder section with different valve lifts of shemen4.

（a）h_v=2 mm   （b）h_v=4 mm   （c）h_v=6 mm   （d）h_v=8 mm
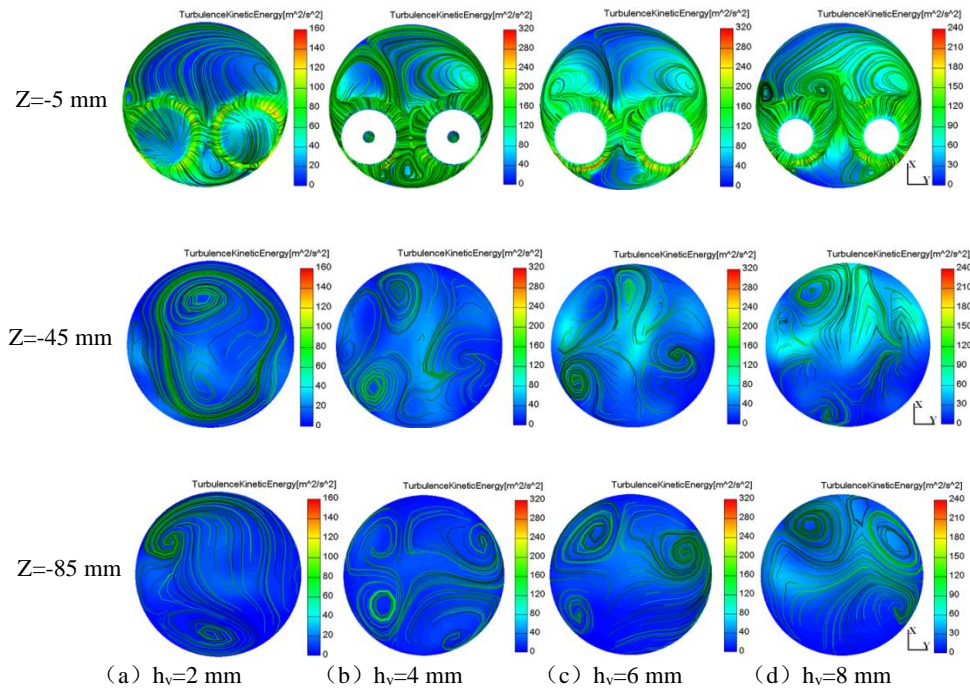
Fig. 17. Turbulent kinetic energy at different cylinder section with different valve lifts of shemen4.

around the valve outlet are formed. With the valve lift increases, two vortexes which rotation in opposite direction below the exhaust valve change from small to large, gradually occupying half of the cylinder.

Comparing the (a), (b), (c) and (d), when the cross-section Z = -35 mm, -65 mm, the swirl motion in cylinder does not form an obvious regularity. The velocity of the air below the intake valve is low, and the velocity below the exhaust valve is higher.

When h_v = 2, 4, 6, and 8 mm, the distribution of turbulent kinetic energy in the cylinder is shown in

Fig. 17. As the figure shown, the turbulent kinetic energy of the air in the cylinder is large, and the energy decay is relatively slow. At the same time, the vortex diffuses continuously with the air flowing to the cylinder bottom, but a single vortex does not integrated. When the valve lift h_v=8 mm, a larger vortex and two equal-sized vortexes converge at the cross-section of Z=-85 mm, and the turbulent energy dissipation is small. The irregular vortexes expand obvious, disappears, and converge gradually in the process of moving from 1/2 stroke cross-section to cylinder bottom.

5. CONCLUSIONS

This work investigates the flow influence of the combined intake ports to itself and in-cylinder by 3D steady-state fluid simulation method and experiment. Some rules on the research are below.

(1) The air flow in the spiral and tangential intake port of the combined intake ports presents certain regularity: when the air flow velocity increases with the valve opening increasing, the slight turbulence occurs at the boss of the valve guide, and even shows viscous flow phenomenon, and the maximum flow velocity at the minimum cross-section of the guide and the helical section is largest.

(2) The small-scale irregular vortexes expand and disappear, and finally converge into a single vortex when the air in cylinder flows from the 1/2 stroke cross-section to the cylinder bottom.

(3) When the air has just flowed into the cylinder, the turbulent energy is very large. After the air entering the cylinder, the flow space expands rapidly and the vortex motion diffuses and merges. The dissipation of turbulent kinetic energy is very significant with the air moving toward to the cylinder bottom.

(4) To master the influence rules of the flow field to combustion, the transient flow fields of the combined intake ports, in-cylinder and the combustion chamber structure should be considered in the future work .

ACKNOWLEDGEMENTS

REFERENCES

Andreatta, É. C., F. A. A. Barbieri, L. L. F. Squaiella and R. Sassake (2008). Intake ports development: Euro IV diesel engine cylinder head *SAE Paper* 2008, 36-0331.

Chunhui, W., L. Jilin, J. Dewen, B. Yuhua and S. Lizhong. (2014). A research on the intake flow and in-cylinder flow field in a four-valve DI diesel engine. *Automotive Engineering* 36 (1), 38-42.

Cui, L., T. Wang, Z. Lu, M. Jia and Y. Sun (2015). Full-Parameter Approach for the Intake Port Design of a Four-Valve Direct-Injection Gasoline Engine. *Journal of Engineering for Gas Turbines and Power* 137(9), 091502.

Deqing, M., W. Zhong and G. Zongying (2002). Experimental study of flow field in the cylinder of a 4-Valve D. I. diesel engine. *Transactions of the Chinese Society of Agricultural* 33(6), 23-25.

Hongwei, M., H. Xiang, Zh. Jinghui, X. Chun long and L. Sheng, (2013). Experimental investigation on engine intake port flow-field visualization. *Chinese Internal Combustion Engine Engineering* 34(1), 46-50.

Hwang, P. W., X. C. Cheng and H. C. Cheng (2016). Influences of Ignition Timing, Spark Plug and Intake Port Locations on the Combustion Performance of a Simulated Rotary Engine. *Journal of Mechanics* 32(5), 579-591.

Kawaguchi, A., T. Aiba, N. Takada and K. Ona (2009). A Robustness-Focused Shape Optimiza tion Method for Intake Ports *SAE Paper* 2009, 01-1777.

Micklow, G. J. and W. D. Gong (2007). Intake and in-cylinder flowfield modeling of a four-valve diesel engine. *Proceedings of the Institution of Mechanical Engineers Part D Journal of Automobile Engineering* 221(11), 1425-1440.

Son, J. W., S. Lee, B. Han and W. Kim (2004). A Correlation between Re-defined Design Parameters and Flow Coefficients of SI Engine Intake Ports. *SAE Technical Papers* 2004, 01-0998.

Stiehl, R., J. Bode, J. Schorr, C. Krüger, A. Dreizler, and B. Böhm (2016). Influence of intake geometry variations on in-cylinder flow and flow–spray interactions in a stratified direct-injection spark-ignition engine captured by time-resolved particle image velocimetry. *International Journal of Engine Research* 17(9), 983-997.

Sun, Y., T. Wang, Z. Lu, L. Cui, M. Jia (2015). The Optimization of Intake Port using Genetic Algorithm and Artificial Neural Network for Gasoline Engines. *SAE Technical Papers* 2015, 01-1353.

Thangavel, V., S. Y. Momula, D. B. Gosala and R. Asvathanarayanan (2016). Experimental studies on simultaneous injection of ethanol–gasoline and n-butanol–gasoline in the intake port of a four stroke SI engine. *Renewable Energy* 91,347-360.

Tianyou, W., L. Daming, Sh. Jie, H. Yiyong, J. Chengji, Zh. Jie, G. Yu, L. Shuliang and J. Zejun (2008). Study of the flow characteristics

of the inlet ports and in-cylinder of internal combustion engine. *Journal of Engineering Thermophysics* 29(4), 693-697.

Yufeng, L., G. Xiaohui, W. Hai, L. shuhang and X. Sidu (2001). Effects of combination and orientation of intake ports on swirl in four-valve DI diesel engines. *Transaction of CSICE* 19(3), 209-214.

Yuguo, G., Y. Zhenzhong, G. Shuman, Q. Chaoju, Ch. Wentao and Zh. Wei (2014). Influence of intake port on mixture formation in hydrogen engine. *Chinese Internal Combustion Engine Engineering* 35(3), 106-111.